AIAA JOURNAL
Vol. 42, No. 3, March 2004

Mechanisms and Responses of a Single Dielectric Barrier Plasma Actuator: Plasma Morphology

C. L. Enloe,* Thomas E. McLaughlin,† Robert D. VanDyken,‡ and K. D. Kachner§
U.S. Air Force Academy, Colorado Springs, Colorado 80840-6222
and
Eric J. Jumper¶ and Thomas C. Corke**
University of Notre Dame, Notre Dame, Indiana 46556-5684

We present simultaneous optical, electrical, and thrust measurements of an aerodynamic plasma actuator. These measurements indicate that the plasma actuator is a form of the dielectric barrier discharge, whose behavior is governed primarily by the buildup of charge on the dielectric-encapsulated electrode. Our measurements reveal the temporal and macroscale spatial structure of the plasma. Correlating the morphology of the plasma and the electrical characteristics of the discharge to the actuator performance as measured by the thrust produced indicates a direct coupling between the interelectrode electric field (strongly modified by the presence of the plasma) and the charges in the plasma. Our measurements discount bulk heating or asymmetries in the structure of the discharge as mechanisms for the production of bulk motion of the surrounding neutral air, although such asymmetries clearly exist and impact the effectiveness of the actuator.

Introduction: Morphology of the Plasma Actuator

THE mechanical configuration of the aerodynamic plasma actuator is shown in Fig. 1. The plasma actuator consists of a set of thin electrodes (in our case made of copper foil tape) arranged spanwise on an aerodynamic surface. One electrode is exposed to the air, while the other is encapsulated in dielectric (Kapton® polyimide tape, in our test articles). The electrodes are offset as shown in the figure and are typically 80 mm wide.

When high ac voltage (5–10-kV amplitude, with frequency in the range of 1–10 kHz) is applied to the electrodes, the unaided eye sees an apparently diffuse plasma discharge, as shown in Fig. 2. The appearance of the plasma is accompanied by a coupling of directed momentum into the surrounding air. This momentum coupling can be effective in substantially altering the flow of air over the actuator surface,[1–9] but, as Fig. 3 shows, it is equally effective in introducing a flow in initially still air.[10]

Although the plasma appears as a relatively uniform diffuse discharge to the unaided eye, optical measurements of the plasma indicate that it is highly structured in both space and time. Figure 4 illustrates the experimental apparatus used to make these measurements. A photomultiplier tube (PMT) was used to observe the bulk plasma with high time resolution. For most of the optical measurements presented here, the PMT was arranged so as to observe approximately one-third of the length of the plasma actuator. For some measurements, a thin slit aperture was interposed between the plasma and the PMT, so that the light observations could be limited to approximately a 1-mm-wide region in the chordwise direction.

We take the light emissions from the plasma actuator as a surrogate for plasma density, assuming that the recombination time of the plasma is short compared to the timescale of the discharge. (This assumption is confirmed by our emissions measurements and is also consistent with the calculations of Vidmar and Stalder,[11] which indicate that we should expect a plasma lifetime on the order of $10^{-8}s$ for our atmospheric-pressure plasmas.) The first observation from the data is that what appears as continuous discharge has considerable temporal structure. Figure 5, for example, shows two cycles of a plasma discharge that turns on and off four times during each cycle of the applied voltage.

The temporal nature of the actuator indicates that this plasma is indeed (as one would have inferred from the electrode configuration) a dielectric barrier discharge (DBD), a configuration about which there is considerable information in the literature[12–23] (see, for example, the review paper by Kunhardt[16]) dating even from the turn of the 20th century.[24] The plasma actuator differs from the most common DBD configuration used in plasma processing in that it employs a single encapsulated electrode and an asymmetric electrode arrangement, but the principles of the discharge are the same. (Gibalov and Pietsch[17] have compared the development of this surface-discharge configuration of the DBD with the more common "volume discharge" configuration.) The most important feature of the DBD is that it can sustain a large-volume discharge at atmospheric pressure without the discharge's collapsing into a constricted arc.

The DBD can maintain such a discharge because the configuration is self-limiting, as illustrated in Fig. 6. To maintain a DBD discharge, an ac applied voltage is required. Figure 6a illustrates the half-cycle of the discharge for which the exposed electrode is more negative than the surface of the dielectric and the insulated electrode, thus taking the role of the cathode in the discharge. In this case, assuming the potential difference is high enough the exposed electrode can emit electrons. Because the discharge terminates on a dielectric surface, however (hence the term "dielectric barrier"), the buildup of surface charge opposes the applied voltage, and the discharge shuts itself off unless the magnitude of the applied voltage is continually increased. This is the explanation of the behavior shown in Fig. 5. At point a in the figure, because of some impedance mismatch in the driving circuit there is a momentary reversal in the slope of the applied waveform. Because the applied voltage is no longer becoming more negative, the discharge shuts off. When, at point b, the applied voltage again resumes its negative course, the discharge reignites and stays ignited until the slope of the voltage waveform goes to zero at approximately $t = 0.4$ ms.

Presented as Paper 2003-1021 at the AIAA 41st Aerospace Sciences Meeting, Reno, NV, 6–9 January 2003; received 7 May 2003; accepted for publication 4 November 2003.

*Professor, Department of Physics. Senior Member AIAA.
†Research Associate, Department of Aeronautics. Associate Fellow AIAA.
‡Research Assistant, Department of Aeronautics.
§Cadet First Class, Department of Physics.
¶Professor, Department of Aerospace and Mechanical Engineering. Fellow AIAA.
**Clark Chair Professor, Department of Aerospace and Mechanical Engineering. Associate Fellow AIAA.

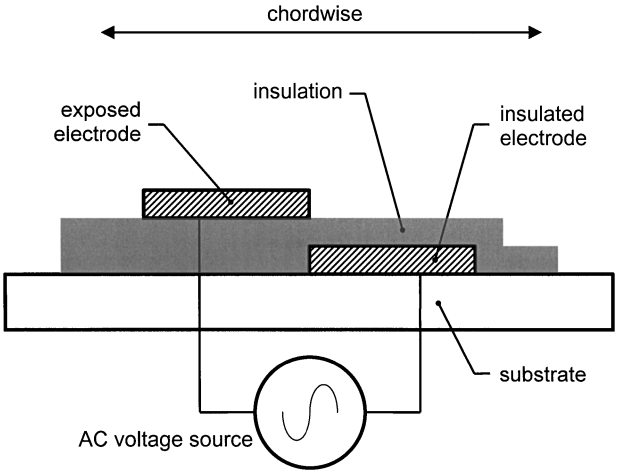

Fig. 1 Plasma actuator is an asymmetric arrangement of electrodes, one of which is insulated, on an aerodynamic surface.

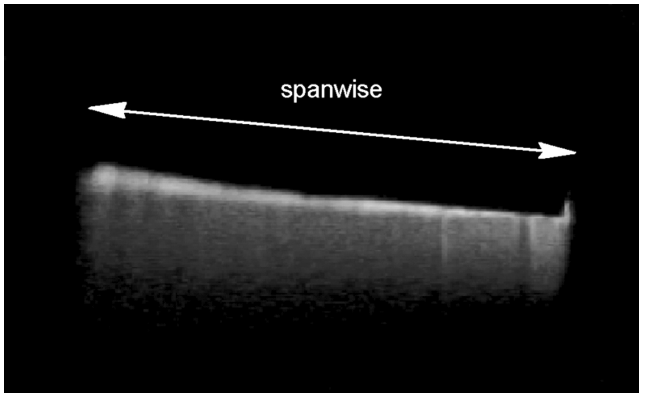

Fig. 2 Plasma actuator in action appears as a diffuse plasma formed on the surface of the dielectric.

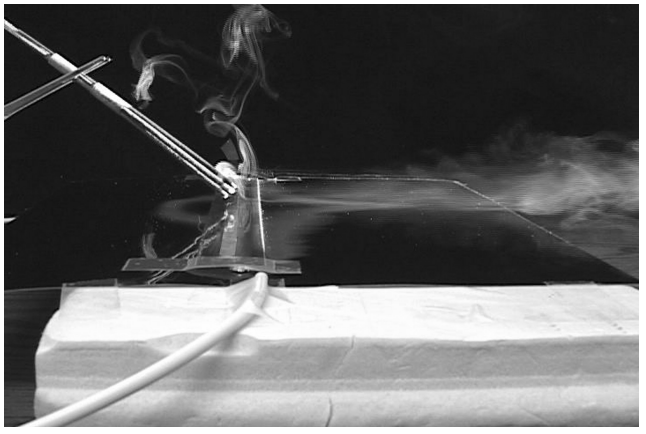

Fig. 3 Plasma actuator can couple momentum into still air along the aerodynamic surface, as illustrated by this flow visualization.

The behavior of the discharge is similar on the opposite half-cycle: a positive slope in the applied voltage is necessary to maintain the discharge. In this half-cycle, the charge available to the discharge is limited to that deposited during the previous half-cycle on the dielectric surface (which now plays the role of the cathode), as shown in Fig. 6b.

This self-limiting behavior caused by charge buildup on the dielectric surface impacts the spatial as well as the temporal structure of the plasma. (We note in passing that the rapid termination of optical emissions with the even momentary reversal of dV/dt in the

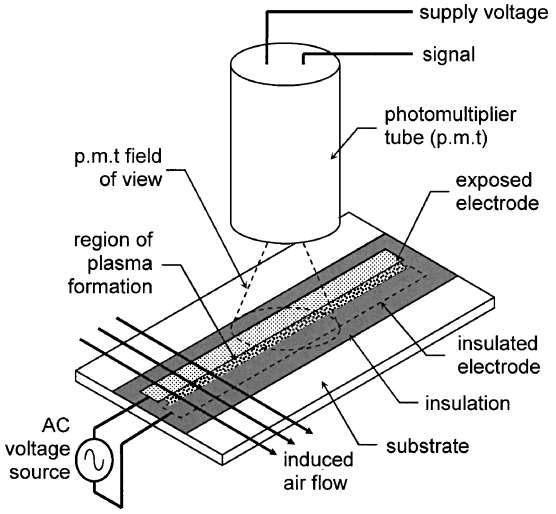

Fig. 4 PMT is used to take fast measurements of the light emission from the plasma actuator.

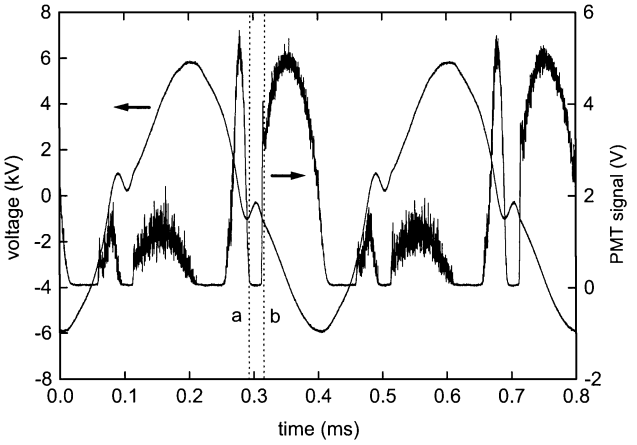

Fig. 5 Light emission from the plasma actuator clearly establishes it as a dielectric barrier discharge.

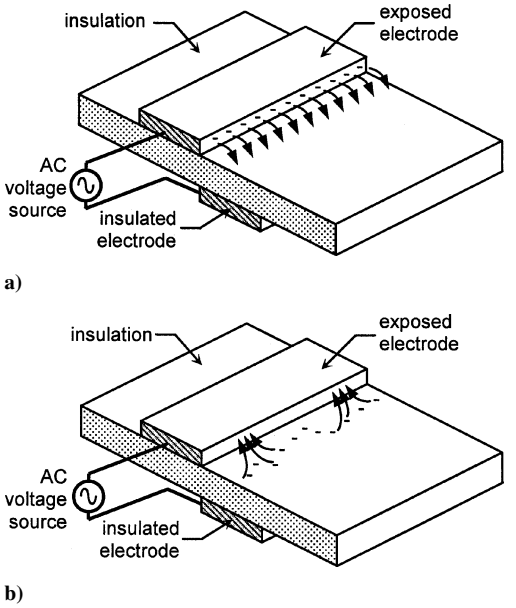

Fig. 6 Dielectric barrier discharge is self-limiting because charge buildup on the dielectric surface opposes the voltage applied across the plasma, when the applied voltage is a) negative going. b) When the voltage reverses, the charge transferred through the plasma is limited to that deposited on the dielectric surface.

applied waveform refutes the claim of Roth et al.[25] that charge builds up in the interelectrode gap because of ion trapping on timescales for a long time compared to the period of the applied voltage. If that were the case, then the ion population would reach an equilibrium value and recombination/deexcitation, with associated light emission, would occur at a relatively uniform rate. In fact, the plasma lifetime is shorter by several orders of magnitude than the timescale of the applied voltage waveform.[11]) It is well established in the literature that although the dielectric barrier discharge consists in many cases of a series of microdischarges[12–23] the same discharge supports other, more diffuse modes,[12,14,16] depending on a number of factors of which the plasma chemistry in the discharge is the chief.[14]

Our optical measurements indicate that there is considerable macroscopic structure spanwise in the plasma actuator discharge. Figure 7 shows one discharge cycle of the plasma actuator with a sinusoidal applied voltage waveform. Both the current through the discharge and the emitted light are shown. The figure shows that the discharge is much more irregular on the positive-going half-cycle than the negative-going. (This behavior is consistent with data in the literature for DBDs with a single dielectric barrier,[17,23] although it is not widely noted; for example, see comments by Gibalov and Pietsch.[17])

Zooming in on the same data on a finer timescale (see Fig. 8) shows that each pulse of light observed on the PMT corresponds to a pulse in the current signal. The reverse, however, is not true: not every current pulse corresponds to a light pulse. The explanation for this observation is straightforward. The PMT's field of view is approximately one-third of the plasma actuator. The current monitor, however, "sees" the entire discharge. Therefore we conclude

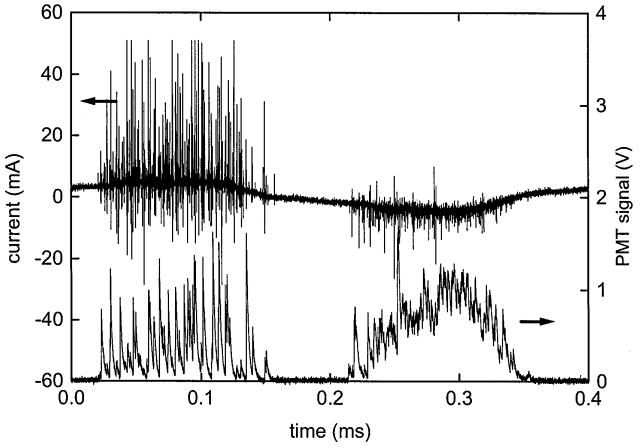

Fig. 7 Emission from the plasma indicate a much more irregular discharge on the positive-going part of the cycle (0.0 to 0.2 ms in this figure) than on the negative-going part (0.2 to 0.4 ms).

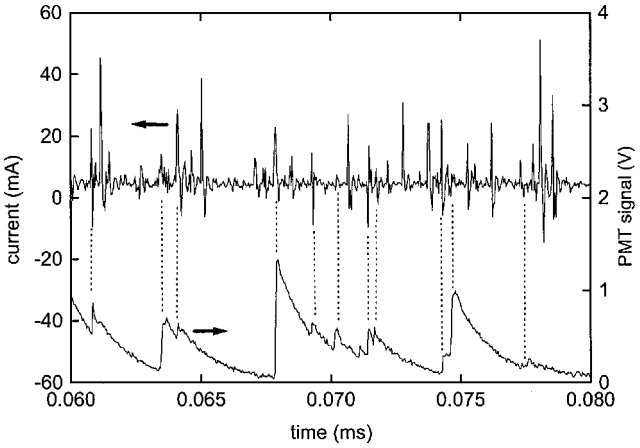

Fig. 8 Detailed look at simultaneous current and light data indicate that the discharge is "patchy" across the entire surface.

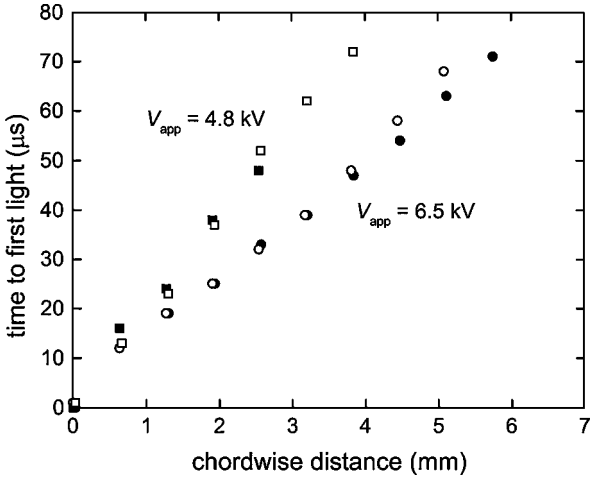

Fig. 9 Time to first light as a function of lateral (chordwise) distance shows that the plasma grows laterally at a constant rate as the discharge progresses. The propagation speed for the negative-going half-cycle (●, ■) is essentially the same as for the positive-going half-cycle (○, □).

that there are discharge events (current pulses) that do not occur in the field of view of the PMT. When the voltage on the exposed electrode is negative-going, the discharge is relatively uniform across the width of the actuator. When the same voltage is positive-going, however, the discharge is "patchy," akin to flashbulbs going off in a stadium. (These measurements are consistent with those made by Gibalov and Pietsch[17] and Wilkinson[1] using fast photography.) This asymmetry in the discharge plays a role in the efficiency of momentum coupling to the flow, as described in the next section.

Optical measurements also indicate that, as Gibalov and Pietsch have noted,[17] the lateral extent of the plasma develops in time. Figure 2 is essentially an open-shutter view of the plasma; the shutter speed is longer than the period of the applied voltage waveform. One would be tempted to interpret this photograph as showing a density gradient in the plasma, with the maximum density nearest the edge of the exposed electrode. This interpretation would be in error, however, as measurements of light emission through a narrow aperture shows. Figure 9 shows the relative time to first light as a function of the lateral position of the aperture. The figure clearly shows that the plasma grows in the lateral (chordwise) direction at a constant rate. Therefore, the fact that the plasma appears brighter nearer the electrode in Fig. 2 corresponds to that location's having emitted for a greater fraction of the discharge cycle, rather than to the presence of a higher plasma density.

From Fig. 9 it is also clear that the propagation speed of the discharge is a function of the amplitude of the applied voltage. The higher the voltage, the faster the discharge spreads along the dielectric surface. Furthermore, the propagation speed of the discharge is essentially the same for both half-cycles of the discharge (negative and positive going) for a given voltage, and in both cases the discharge ignites at the edge of the exposed dielectric and propagates downstream along the dielectric surface. This level of symmetry in the structure of the discharge refutes the model proposed by Shyy et al.,[26] which implies that electrons leaving the dielectric surface would have energy sufficient to ionize the background only when they near the exposed electrode and proceeds to attribute the action of the actuator to such asymmetry in the discharge. On the contrary, although there is a difference in the transverse (spanwise) structure of the plasma between half-cycles of the discharge the lateral (chordwise) extent and development of the plasma is essentially the same.

Electrical Circuit Analysis of the Plasma Actuator

Understanding that the plasma actuator is in fact a dielectric barrier discharge makes it possible to analyze the discharge with a lumped-element circuit model. The simplest circuit model that one can use is shown in Fig. 10. The key to building an applicable model

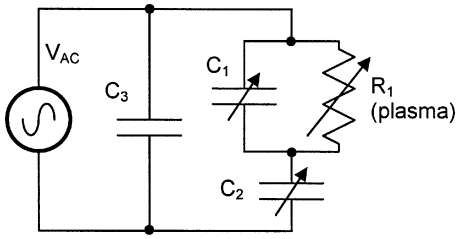

Fig. 10 Lumped-element circuit model of the plasma actuator takes into account the charging of the dielectric surface as a virtual electrode.

is understanding that in addition to the two physical electrodes in the actuator the exposed surface of the dielectric acts as a virtual electrode as it collects charge. Therefore there are three capacitive elements in the circuit model shown in Fig. 10. The capacitor C_1 represents the capacitance between the exposed physical electrode and the virtual electrode on the dielectric surface. The capacitor C_2 represents the capacitance between the virtual electrode and the encapsulated physical electrode. Because the electrodes are offset, it is also necessary to include a capacitance C_3 because some field lines connect the physical electrodes directly. (This capacitance provides a parallel path for additional displacement current in the circuit, but does not affect the discharge itself.)

Because, as we have shown in the preceding section, the chordwise extent of the plasma changes during the discharge, the values of C_1 and C_2 will as well; hence, they are indicated in Fig. 10 as variable elements. It is useful to consider the average capacitance values for these elements and to realize that this average depends on the amplitude of the applied voltage.

The plasma, shown as a resistance R_1 in the circuit model, is the single dissipative element in the circuit. The plasma does not exist during the entire discharge, and so we indicate R_1 as a variable resistance value. When the absolute value of the potential difference across C_1 exceeds a threshold value, the plasma ignites, and the resistance R_1 drops from an effectively infinite, open-circuit value, to a low value. When the absolute value of the potential difference falls below another threshold, the discharge quenches, and R_1 returns to its open-circuit value. The voltage source V_{AC} must be, by the nature of the DBD plasma, an ac source in order for the discharge to be sustained.

Knowing that the spatial structure of the plasma actuator discharge is asymmetric, we investigated the importance of this asymmetry by applying two different asymmetric voltage waveforms, mirror images of each other, to the plasma. Both were sawtooth waveforms, in one case the positive sawtooth, where the voltage applied to the exposed electrode had a large positive slope and a smaller negative slope. The negative sawtooth had its faster transition when negative-going and its slower when positive going. We monitored voltage and current waveforms simultaneously and integrated the power dissipated in the plasma directly from those waveforms. (Each averaged over a number of cycles to average out the noise, as shown in Fig. 8.) Figures 11 and 12 show the voltage and current waveforms, respectively. On the gross scale, the light emission from the plasma in each case (shown in Figs. 13 and 14) seem to reflect the fact that the shape of the positive- and negative-sawtooth waveforms are essentially the same. If we look in detail, however, we see that the asymmetry of the discharge noted earlier also appears in these measurements. For each waveform, the negative-going portion of the waveform (Figs. 13b and 14a) produces the more uniform discharge. The positive-going portion (Figs. 13a and 14b) produces the more irregular discharge, consistent with the results shown in Fig. 5.

The importance of the difference in the structure of these two plasmas is evident when we measure the effect that each has on the surrounding air. We gauge the actuator's effectiveness by measuring the thrust it produces when operated in initially still air. The arrangement used to make this measurement is shown in Fig. 15. The actuator is mounted on a lever arm, and the thrust it produces is measured on a mass balance at the opposite end of the arm.

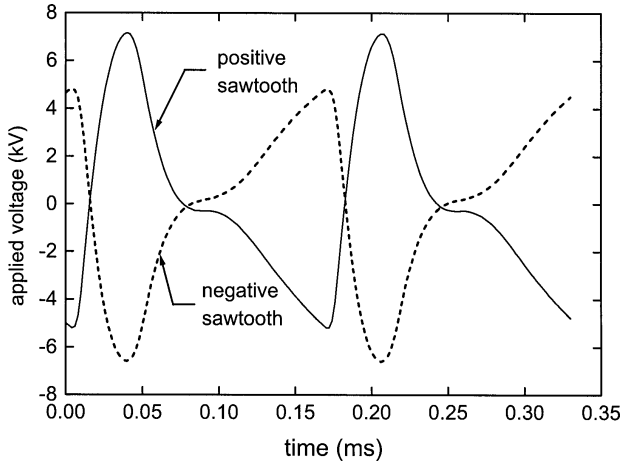

Fig. 11 Positive- and negative-sawtooth voltage waveforms were applied to the plasma actuator to investigate the effects of discharge asymmetry.

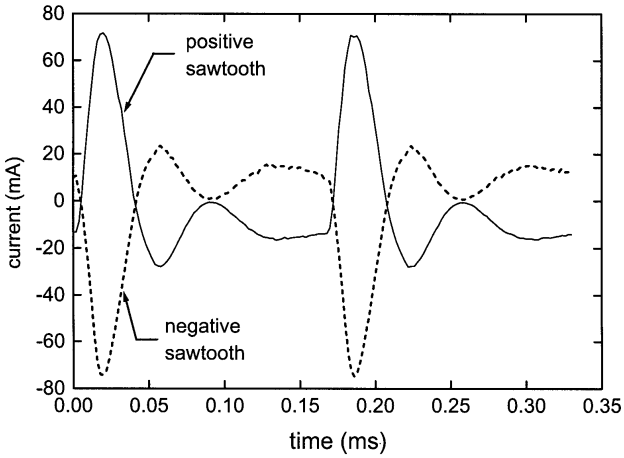

Fig. 12 Positive- and negative-sawtooth current waveforms were applied to the plasma actuator to investigate the effects of discharge asymmetry.

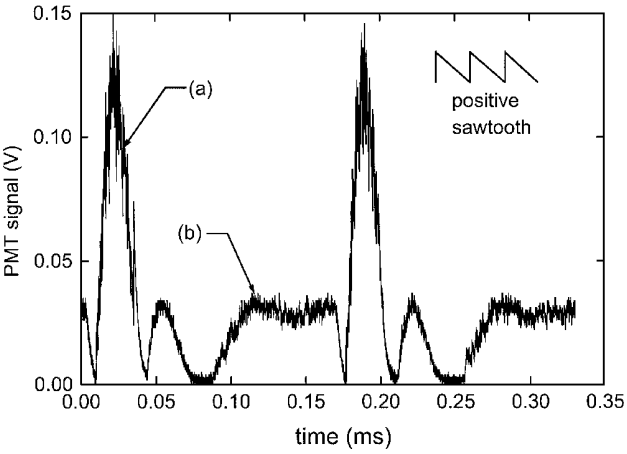

Fig. 13 Light emission from the plasma actuator for the case of the positive sawtooth applied voltage waveform.

One often discussed (but rarely referenced) theory of the operation of the plasma flap attributes its effect to heating of the air. If this theory is correct, then either polarity of the sawtooth waveform should be equally effective, given the same average power dissipated by the plasma. In fact, this is not the case. Figure 16 shows thrust vs dissipated power for both the positive- and negative-sawtooth waveforms. As the figure shows, there is a considerable difference between the two waveforms. The positive-sawtooth waveform, which

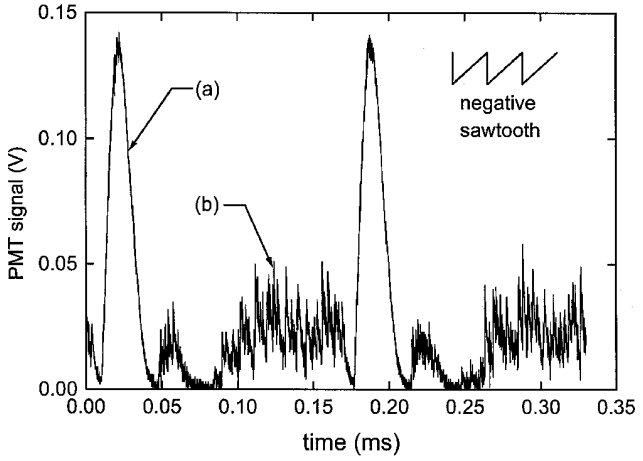

Fig. 14 Light emission from the plasma actuator for the case of the negative sawtooth applied voltage waveform.

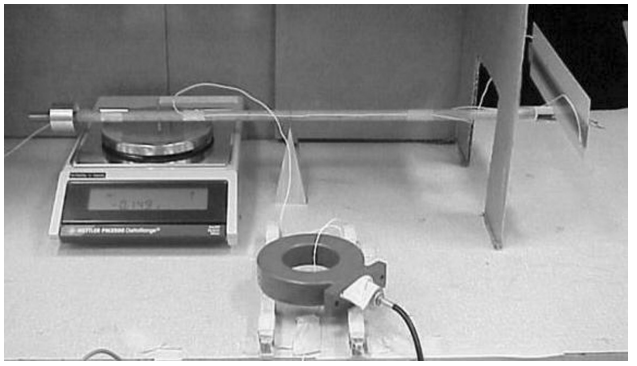

Fig. 15 Effect of the plasma actuator on still air is determined by measuring the thrust it produces with a mass balance.

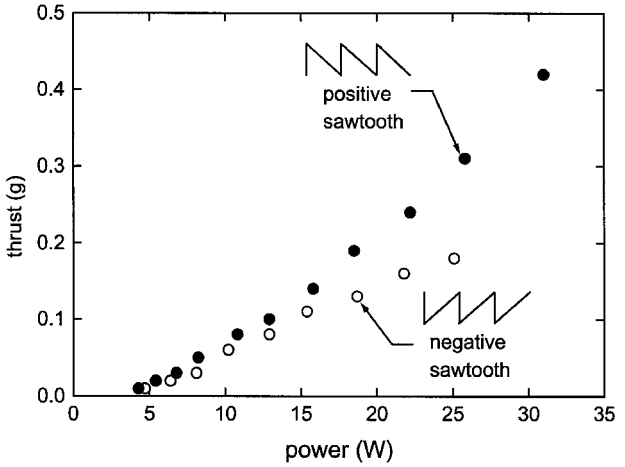

Fig. 16 Thrust vs dissipated power for both positive- and negative-sawtooth voltage waveforms applied to the plasma actuator.

has a higher negative-going duty cycle and therefore produces a more diffuse plasma for a greater fraction of the discharge cycle, produces the greater thrust. The negative-sawtooth waveform, in contrast, produces a more irregular plasma for a greater fraction of the discharge cycle and is less efficient in coupling momentum into the flow for a comparable dissipated power. Therefore, we can disregard bulk heating as the primary mechanism of the operation of the plasma flap. Finally, we note that the power dissipation as a function of amplitude of the applied voltage is consistent with the morphology of the plasma previously noted. As Fig. 10 shows, when the plasma ignites (effectively shorting out the capacitance

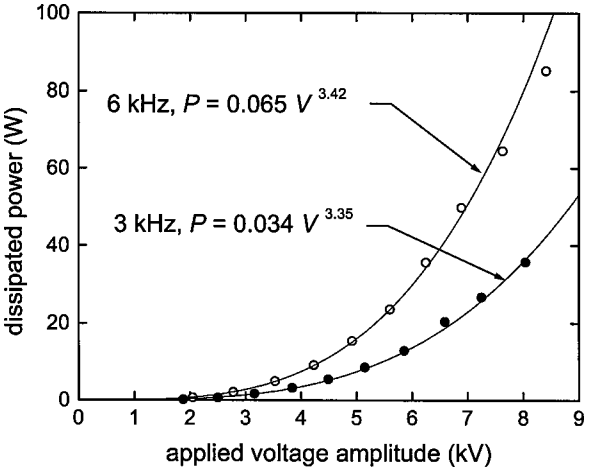

Fig. 17 Power dissipated in the plasma goes as $V_{AC}^{7/2}$, indicating that the average value of the lumped circuit elements depends on the voltage applied to the circuit.

C_1) it forms part of a voltage divider. The impedance Z_2 of the other element of the divider, the capacitance C_2, depends on the frequency of the applied waveform $Z_2 = -i/\omega C_2$, but for a fixed frequency we would expect power dissipated to go as V_{AC}^2 if C_2 is constant. As Fig. 17 shows, however, power dissipated in the plasma goes approximately as $V_{AC}^{7/2}$. This is consistent with one or both of two situations: 1) an average capacitance C_2 that increases with increasing applied voltage or 2) an average resistance R_1 that decreases with increasing applied voltage. As we have seen from the preceding section, the higher the voltage, the faster the plasma sweeps over the surface of the dielectric, meaning that the average area of the virtual electrode atop the dielectric, and hence the value of the capacitance C_2, increases with increasing V_{AC}. In numerical simulations of the circuit, to reproduce the output waveforms with reasonable fidelity it is necessary to introduce a variable resistance that decreases with voltage just as these power traces imply. We intend to investigate possible techniques[27] to directly diagnose the temperature and density of the plasma to further confirm this issue.

Electric Forces on the Plasma Actuator

The direct measurement of thrust from the plasma actuator, although a simple measurement, is instructive in terms of the mechanism involved. To measure thrust on the mass balance, as shown in Fig. 15, there must be a mechanical coupling between the moving air and the actuator. Because this coupling only occurs when the plasma is present, we can infer that the plasma is the intermediary. The way that the plasma can couple force into the actuator is via the electric field interactions with the charged particles in the plasma. Essentially, the charges in the plasma "push" on both the background gas and the image charges in the electrodes, completing the chain of forces leading to a measurement of thrust.

We have asserted that although the structure of the plasma is different in each half-cycle of the DBD discharge in the plasma actuator it is not this asymmetry that appears to drive the direction of the induced airflow, as Shyy has suggested.[26] To further test this, we applied sawtooth waveforms to a different configuration of electrodes, as shown in Fig. 18. In this case, the electrodes were made of insulated magnet wire, so that unlike the configuration shown in Fig. 1 neither electrode was the preferential electron emitter. The geometric asymmetry in the arrangement, however, was maintained.

With both electrodes encapsulated, this arrangement of the plasma actuator was much less efficient at producing plasma and therefore at producing thrust, and so it was not feasible to measure thrust directly. Instead, we used smoke as a flow-visualization tool, with the results shown in Fig. 19. As the figure shows, the direction of the induced airflow was the same, to the right, regardless of the polarity of the waveform. Therefore, it was clearly the geometry of the electrodes that determined the direction of the flow.

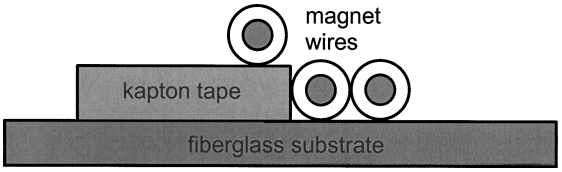

Fig. 18 Plasma actuator with both electrodes encapsulated was fabricated to investigate whether the asymmetry in the discharge was the driver in the direction of the airflow.

Fig. 19 Airflow is induced in the same direction—as shown, in this case, by smoke flowing to the right—irrespective of the polarity of the applied waveform in the case of the actuator with both electrodes encapsulated. In this figure the electrodes are arranged vertically.

With such an asymmetric arrangement of the electrodes, the electric field will similarly be highly structured even in the absence of plasma. Because of the mobility of the charges (ions and electrons) once the plasma ignites, the plasma will further enhance asymmetries in the electric field structure. In general, the effect of having the plasma present requires a detailed calculation, but some insight can be gleaned by considering a specific case of an asymmetric electrode arrangement in the presence of a plasma.

Conclusions

Based on electrical and optical measurements of the plasma, the aerodynamic plasma actuator is clearly identified as a dielectric barrier discharge. The discharge exhibits gross structure both in space and time. Because this structure clearly affects the efficiency of momentum coupling into the neutral air, bulk heating can be discounted as a mechanism for this interaction. The fact that the asymmetry in the discharge does not, however, control the direction of the momentum coupling indicates that an interaction of the plasma with the applied electric field in the discharge is responsible for the body force and subsequent momentum transfer to the neutral fluid through plasma-neutral collisions. The strong influence that the structure of the plasma has on the momentum transfer suggests that a detailed, multidimensional model of the actuator will be necessary to unwrap the physics of the problem and enable accurate predictions of its performance.

Acknowledgments

The authors gratefully acknowledge the support provided by John Anttonen of the Munitions Directorate of the U.S. Air Force Research Laboratory, Eglin Air Force Base, Florida.

References

[1]Wilkinson, S., "Investigation of an Oscillating Surface Plasma for Turbulent Drag Reduction," AIAA Paper 2003-1023, Jan. 2003.

[2]Post, M., and Corke, T., "Separation Control on High Angle of Attach Airfoil Using Plasma Actuators," AIAA Paper 2003-1024, Jan. 2003.

[3]Ashpis, D., and Hultgren, L., "Demonstration of Separation Delay with Glow Discharge Plasma Actuators," AIAA Paper 2003-1025, Jan. 2003.

[4]List, J., Byerley, A., McLaughlin, T., and VanDyken, R., "Using Plasma Actuator Flaps to Control Laminar Separation on Turbine Blades in a Linear Cascade," AIAA Paper 2003-1026, Jan. 2003.

[5]Huang, J., Corke, T., and Thomas, F., "Plasma Actuators for Separation Control of Low Pressure Turbine Blades," AIAA Paper 2003-1027, Jan. 2003.

[6]Corke, T. C., Jumper, E. J., Post, M. L., Orlov, D., and McLaughlin, T. E., "Application of Weakly-Ionized Plasmas as Wing Flow-Control Devices," AIAA Paper 2002-0350, Jan. 2002.

[7]Roth, J. R., Sherman, D. M., and Wilkinson, S. P., "Electrohydrodynamic Flow Control with a Glow-Discharge Surface Plasma," *AIAA Journal*, Vol. 38, 2000, pp. 1166–1172.

[8]Corke, T. C., and Matlis, E., "Phased Plasma Arrays for Unsteady Flow Control," AIAA Paper 2000-2323, Jan. 2000.

[9]Roth, J. R., Sherman, D. M., and Wilkinson, S. P., "Boundary Layer Flow Control with a One Atmosphere Uniform Glow Discharge Surface Plasma," AIAA Paper 98-0328, Jan. 1998.

[10]Enloe, C. L., "Optical and Electrical Measurements of a Highly Asymmetric Dielectric Barrier Discharge for Flow Control on Aerodynamic Surfaces," American Physical Society, 55th Annual Gaseous Electronics Conference, Paper QWP 87, Oct. 2002.

[11]Vidmar, R. J., and Stalter, K. R., "Air Chemistry and Power to Generate and Sustain Plasma: Plasma Lifetime Calculations," AIAA Paper 2003-1189, Jan. 2003.

[12]Mangolini, L., Orlov, K., Kortshagen, U., Heberlein, J., and Kogelschatz, U., "Study of Different Discharge Regimes in a Dielectric Barrier Discharge: Electrical and Optical Characterization," American Physical Society, 55th Annual Gaseous Electronics Conference, Paper NR2.003, Oct. 2002.

[13]Kang, W. S., Kim, Y., and Hong, S. E., "Spatio-Temporal Images of Single Streamer Propagation in Dielectric Barrier Discharge," *IEEE Transactions on Plasma Science*, Vol. 30, 2002, pp. 166, 167.

[14]Gherardi, N., and Massines, F., "Mechanisms Controlling the Transition from Glow Silent Discharge to Streamer Discharge in Nitrogen," *IEEE Transactions on Plasma Sciences*, Vol. 29, 2001, pp. 536–544.

[15]Liu, S., and Neiger, M., "Excitation of Dielectric Barrier Discharges by Unipolar Submicrosecond Square Pulses," *Journal of Physics D: Applied Physics*, Vol. 34, 2001, pp. 1632–1638.

[16]Kunhardt, E. E., "Generation of Large-Volume, Atmospheric-Pressure, Nonequilibrium Plasmas," *IEEE Transactions on Plasma Science*, Vol. 28, 2000, pp. 189–200.

[17]Gibalov, V. I., and Pietsch, G. J., "The Development of Dielectric Barrier Discharges in Gas Gaps and on Surfaces," *Journal of Physics D: Applied Physics*, Vol. 33, 2000, pp. 2618–2636.

[18]Steinle, G., Neundorf, D., Hiller, W., and Pietralla, M., "Two-Dimensional Simulation of Filaments in Barrier Discharges," *Journal of Physics D: Applied Physics*, Vol. 32, 1999, pp. 1350–1356.

[19]Massines, F., Rabehi, A., Decomps, P., Ben Gadri, R., Segur, P., and Mayoux, C., "Experimental and Theoretical Study of a Glow Discharge at Atmospheric Pressure Controlled by Dielectric Barrier," *Journal of Applied Physics*, Vol. 83, 1998, pp. 2950–2957.

[20]Xu, X., and Kushner, M. J., "Multiple Microdischarge Dynamics in Dielectric Barrier Discharges," *Journal of Applied Physics*, Vol. 84, 1998, pp. 4153–4160.

[21]Li, J., and Dhali, S. K., "Simulation of Microdischarges in a Dielectric-Barrier Discharge," *Journal of Applied Physics*, Vol. 82, 1997, pp. 4205–4210.

[22]Falkenstein, Z., and Coogan, J. J., "Microdischarge Behavior in the Silent Discharge of Nitrogen-Oxygen and Water-Air Mixtures," *Journal of Physics D: Applied Physics*, Vol. 30, 1997, pp. 817–825.

[23]Pashaie, B., Dhali, S. K., and Honea, F. I., "Electrical Characteristics of a Coaxial Dielectric Barrier Discharge," *Journal of Physics D: Applied Physics*, Vol. 27, 1994, pp. 2107–2110.

[24]Wharburg, E., *Annals of Physics*, Vol. 13, 1904, pp. 464–476.

[25]Roth, J. R., Tsai, P. P., Liu, C., Laroussi, M., and Spence, P. D., "One Atmosphere, Uniform Glow Discharge Plasma," U.S. Patent 5,414,324, 1995.

[26]Shyy, W., Jayaraman, B., and Anderson, A., "Modeling of Glow-Discharge-Induced Fluid Dynamics," *Journal of Applied Physics*, Vol. 92, 2002, pp. 6434–6443.

[27]Park, J., Henins, I., Herrmann, H. W., and Selwyn, G. S., "Neutral Bremsstrahlung Measurement in an Atmospheric-Pressure Radio Frequency Discharge," *Physics of Plasmas*, Vol. 7, 2000, pp. 3141–3144.

M. Sichel
Associate Editor